BOREAL ENVIRONMENT RESEARCH 30: 93–109
ISSN 1797-2469 (online)

Helsinki 10 April 2025

Less frequent but more intense summertime precipitation in Finland: results from a convection-permitting climate model

Laura Utriainen*, Meri Virman, Anton Laakso, Jenna Ritvanen, Kirsti Jylhä, and Joonas Merikanto

Finnish Meteorological Institute, Erik Palmenin aukio 1 00560 Helsinki Finland
**corresponding author's e-mail: laura.utriainen@fmi.fi*

Received 12 Jul. 2024, final version received 24 Jan. 2025, accepted 28 Feb. 2025

Utriainen L., Virman M., Laakso A., Ritvanen J., Jylhä K. & Merikanto J. 2025: Less frequent but more intense summertime precipitation in Finland: results from a convection-permitting climate model. *Boreal Env. Res.* 30: 93–109.

Changes in short-term precipitation events have significant local impacts as a result of climate change, yet are poorly captured by coarse-resolution global climate models. We analyse the projected changes in warm season precipitation events in Finland from a convection-permitting regional climate model HARMONIE-Climate, operating at 3-kilometer resolution. Realistic modeled precipitation characteristics are verified against multiple observational datasets for 1986–2018, and projected changes in precipitation events are analyzed until 2041–2060 and 2081–2100. We show that as climate change proceeds the frequency of precipitation events above 2 mm h^{-1} increases, while the frequency of lower intensity events decreases. In a strong climate change scenario (RCP8.5), extremely heavy precipitation exceeding 20 mm h^{-1} will become twice to three times as common (three to six times) in 2041–2060 (2081–2100) compared to 1986–2005, while simultaneously the total number of wet hours is projected to decrease by 12–16% (18–25%).

Introduction

Climate change directly affects the global hydrological cycle (Douville *et al.* 2021). A significant concern about climate change is how it will alter Earth's regional precipitation patterns and thus impact human societies and natural ecosystems. In Europe, hazards associated with precipitation have become increasingly frequent, resulting in losses and damage to property, infrastructure, food systems, and public health (Bednar-Friedl *et al.* 2022).

The Nordic region has already undergone increases in observed daily and sub-daily heavy rainfall (Dyrrdal *et al.* 2021; Rutgersson *et al.* 2022; Olsson *et al.* 2022; Tamm *et al.* 2023) and this trend is projected to continue (Lehtonen *et al.* 2019; Christensen *et al.* 2022; Climate Change (IPCC) 2023; Lind *et al.* 2023). In Finland, the same pattern is evident for daily precipitation (Venäläinen *et al.* 2009; Lehtonen *et al.* 2014; Irannezhad *et al.* 2017; Pedretti *et al.* 2019), and the 5-year return level of observed daily precipitation has increased by up to 10 percent in the majority of observation stations between 1969 and 2020 (Dyrrdal *et al.* 2021). Furthermore, Coupled Model Intercomparison Project (CMIP) Phase 6 global climate models (GCMs) project a slight increase in summertime mean monthly

Editor in charge of this article: Antti Arola
https://doi.org/10.60910/ber2025.xv04-3n48

precipitation in Finland in the future, although some of the models disagree on the direction of the change for the precipitation totals (Ruosteenoja *et al.* 2021). Generally, it is estimated that the rise in total precipitation is associated with an increase in more frequent heavy, short-duration precipitation events, while the increase in average intensity is less notable (Fischer *et al.* 2014; Myhre *et al.* 2019; Lind *et al.* 2023).

Various sectors, including transportation, urban planning, water management, agriculture, and forestry, depend on information about changes in future precipitation patterns and intensities at a regional scale. This enables them to develop more effective policies and practices to manage the increased risk of heavier rainfall (Madsen *et al.* 2018). Short-duration, high-intensity precipitation events typically result from deep moist convection (Emanuel 1994), which climate models with spatial resolution coarser than 4 km are not able to explicitly resolve. Thus, to achieve assessments on both short-duration precipitation events and precipitation projections for regional needs, there is a need to downscale from coarse GCMs to higher spatial resolution. Using convection-permitting regional climate models on the kilometer scale enables explicitly resolve deep convection and enhance spatial accuracy (Kendon *et al.* 2012; Prein *et al.* 2015; Lucas-Picher *et al.* 2021).

Recently, convection-permitting climate model simulations made with the regional HARMONIE-Climate model (HCLIM), run at 3 km resolution, have become available over Fennoscandia (Lind *et al.* 2020). HCLIM has been evaluated against a number of different observation and reanalysis datasets over Northern Europe by Lind *et al.* (2020, 2023). Furthermore, Médus *et al.* (2022) have demonstrated HCLIM's added value in simulating warm season's extreme daily precipitation in the Nordic region. However, due to the lack of consistent and long continuous sub-daily precipitation data in Finland, a comparison of hourly-scale precipitation in Finland was not made in that study, but the added value for extreme sub-daily precipitation was shown elsewhere in the Nordic region.

With HCLIM, Lind *et al.* (2023) projected that both daily and sub-daily intense precipitation events will become more frequent at the expense of low-intensity events in Fennoscandia. Their study encompassed a variety of topographies, including Scandinavian mountains, the Atlantic coast, and flat areas such as Denmark and southern Sweden.

In this study, we first continue and complement the previous evaluation of HCLIM's precipitation distribution in Finland by making a comparative analysis of hourly and daily precipitation between HCLIM and several observational datasets over Finnish land areas. The goal is to confirm the model's capability to reasonably replicate the mean precipitation characteristics and variability seen in observations. Then, we extend the analysis presented in Lind *et al.* (2023) to investigate projected changes in rapid, hourly precipitation characteristics over Finnish land areas in greater detail. The main goal of this study is to provide more precise regional information of the projected future changes in sub-daily precipitation and in the frequencies of different precipitation intensities. Special attention is paid to projected changes in heavy precipitation events, defined by the thresholds used in the alert classifications of the Finnish Meteorological Institute (FMI), where in heavy rain is identified at a threshold of 7 mm h^{-1}, and the national alert level for potentially dangerous rainfall is set at 20 mm h^{-1} (FMI: Heavy Rain Warning, n.d.) .

The structure of the paper is as follows: the Data section describes the data, including the model data and the observational datasets; and the Methods section describes the methodology used in this study. The Results section presents the results in two main parts. In the first part, a comparative analysis of precipitation in Finland is performed between the model experiments and observations to evaluate the model's performance. The second part examines projected future changes in summertime precipitation in Finland under different scenarios, analyzing changes in monthly precipitation intensity and wet hour precipitation intensity, the occurrence of wet hours, and shifts in hourly precipitation intensities. Finally, the last section provides a discussion of the findings and the conclusions drawn from this study.

Data

HCLIM

We analyzed climate model data, at 3 km spatial resolution, produced by the regional climate model HCLIM cycle 38 (HCLIM38) and generated in the Nordic Convection Permitting Climate Projections project (NorCP; Lind *et al.* (2020)). We use the simulations made with the HCLIM38-AROME configuration that employs non-hydrostatic dynamics and includes explicitly resolved deep convection. In the NorCP project, the experiments were first conducted with the numerical weather prediction limited area model ALADIN (Termonia *et al.* 2018) with a spatial resolution of 12 km, covering a domain that includes Northern Europe, parts of Central Europe, and the Eastern North Atlantic. Then, the ALADIN simulations were downscaled using the small-scale numerical weather prediction model AROME with a spatial resolution of 3 km over Fennoscandia (see the model domain in Supplementary Information Fig. A1). The boundary conditions for the ALADIN simulations were derived from the ERA-Interim reanalysis (Dee *et al.* 2011) for the hindcast simulation (1998–2018), and from two global climate models participating in the CMIP5 experiment, EC-Earth2 (Hazeleger *et al.* 2010) and GFDL-CM3 (Donner *et al.* 2011), for the historical (1986–2005), mid-century (2041–2060), and late century (2081-2100) periods. The temperature of the lakes is simulated by the FLake lake model (Mironov *et al.* 2010). This model is a two-layer parametric model of the changing temperature profile, which relies on the integral energy budgets calculated for each of the two layers. The details of HCLIM38 are elaborated in Belusić *et al.* (2020), and for a detailed description of the simulation methodology, see Lind *et al.* (2020) and Médus *et al.* (2022). For simplicity, we refer to the HCLIM38-AROME configuration used here as HCLIM.

The future scenarios downscaled in the NorCP project were the Representative Concentration Pathways (RCPs; Moss *et al.* 2010; Van Vuuren *et al.* 2011) with an associated radiative forcing of 8.5 Wm^{-2} (RCP8.5) at the end of the 21st the century for GFDL-CM3, and 8.5 Wm^{-2} and 4.5 Wm^{-2} (RCP4.5) for EC-Earth2. EC-Earth2 aligns closely with the average predictions of the CMIP5 ensemble, while GFDL-CM3 projects a more pronounced climate shift, projecting higher rise of global mean temperature and faster reduction in Arctic sea-ice cover throughout the 21st century, causing more rapid changes in the Nordic region (Lind *et al.* 2023). In this study, we refer to the HCLIM experiments using boundary conditions from ERA-Interim, EC-Earth2, and GFDL-CM3, as HCLIM-erai, HCLIM-ece, and HCLIM-gfdl, respectively. We note that the climatology in the parent GCMs used in the HCLIM-ece and HCLIM-gfdl simulations was not nudged but was based on free-running CMIP5 modeling design (Taylor *et al.* 2012), so the simulated years should only represent typical years for the simulated period. In contrast, the HCLIM-erai simulation obtained their boundary conditions from the ERA-Interim reanalysis, and hence the simulated years represent the actual climatology of the years. The different HCLIM simulations are presented in Table 1.

Observational data

The observations, derived from FMI's observational network and used in the comparative analysis with HCLIM, included hourly *in-situ* gauge observations for three different time periods, as well as Finland's weather radar data, and gridded daily precipitation data at 1 km resolution. The observational datasets are presented in Table 2.

In-situ gauge observations

We analyze *in-situ* gauge observations of hourly precipitation from surface weather stations in Finland. To take into account the different time periods covered by the historical HCLIM simulations (Table 1) and weather radar data (see Table 2), as well as the inconsistent amount of observation stations over time, the gauge observations were split into three datasets (Gauge dataset 1, 2 and 3). These Gauge datasets cover different time periods and include gauge observations from different number of stations, which have

records of hourly precipitation measurements either covering partly or completely the modeled period (Table 2). First, Gauge dataset 1 is compared against HCLIM-erai, and it covers the entire temporal range of that simulation (1998–2018) and includes data from the 119 weather stations that recorded hourly precipitation during that period. Second, Gauge dataset 2 is used in comparison with HCLIM-erai and weather radar data and it includes observations from 97 stations. That dataset covers only a six year period because the suitable weather radar data for our analysis was available only for the years 2013–2018. Finally, Gauge dataset 3 is compared with HCLIM-ece and HCLIM-gfdl, it covers the years 1996–2005 and includes 36 stations. Note that Gauge dataset 3 does not cover the full period available for the HCLIM-ece and HCLIM-gfdl simulations, as to the authors' knowledge, no hourly gauge observations have been digitized prior to 1996 in Finland. The hourly precipitation in the gauge datasets has been measured by

Table 1. The HCLIM simulations used in this study. "Boundaries" denotes the GCM and/or reanalysis used as boundary condition for the HCLIM simulations. "Gridded data" refers to the gridded daily mean precipitation intensity and temperature data of FMI (which are part of the NGCD product). T, PrWH, and PrMon denote the mean temperature, mean wet hour precipitation intensity, and mean monthly precipitation intensity in June–September (JJAS) in Finland, calculated from the HCLIM simulations and, in case of T and PrMon, from the gridded daily data. The apparent hydrological sensitivity, η_a, is defined as the percentage change in mean monthly precipitation per degree Celsius of monthly future warming, relative to the historical period 1986-2005. The spatial distributions of T, PrWH and PrMon are shown in the Supplementary Information Figures D1-D3.

Dataset and period	Boundaries and Scenario	T (°C)	PrWH (mm h^{-1})	PrMon (mm $month^{-1}$)	η_a (% $°C^{-1}$)
HCLIM-erai	ERA-Interim				
1998—2018	historical	12.1	0.93	70.1	
HCLIM-ece	EC-Earth2				
1986—2005	historical	10.1	0.81	64.6	
2041—2060	RCP4.5	11.7	0.87	62.9	—1.5
	RCP8.5	12.4	0.96	64.2	—0.1
2081—2100	RCP4.5	12.3	0.94	67.0	1.8
	RCP8.5	14.5	1.07	68.9	1.5
HCLIM-gfdl	GFDL-CM3				
1986—2005	historical	9.0	0.73	69.8	
2041—2060	RCP8.5	13.0	0.95	79.3	3.5
2081—2100	RCP8.5	16.3	1.18	82.0	2.4
Gridded data					
1986—2005		12.6		66.5	
1998—2018		13.1		68.0	

Table 2. Observational datasets used for the comparison of HCLIM and observed precipitation data. The column "Stations/Domain" denotes, for the gauge datasets, the number of stations that had a record of hourly gauge precipitation measurements either covering partly or completely the modeled period. For the radar and gridded datasets, it indicates the study domain. We lack radar observations from the northernmost part of Lapland, and there are also gaps in radar data near the eastern border of Finland. The locations of the *in-situ* gauge observational stations for each Gauge dataset are provided in Supplementary Information Fig. B1.

Dataset	Period	Stations/Domain
Gauge dataset 1	1998—2018	119
Gauge dataset 2	2013—2018	97
Gauge dataset 3	1996—2005	36
Radar observations	2013—2018	Finland, except northernmost Lapland
Gridded observations	1986—2005	Finland

a weighing gauge "Vaisala FD12P" starting from 4 July 1996, and by a weighing gauge "Vaisala VRG" starting from 31 January 2006, with the newer instrument having an enhanced accuracy; nevertheless, we stress that even the more recent gauge observations are prone to significant measurement inaccuracies. For the locations of the weather stations for each gauge dataset see Fig. B1 in Supplementary Information.

Radar observations

We used 6 years of single-polarization radar rainfall measurements between 2013–2018 from the Finnish national weather radar network (Saltikoff *et al.* 2010). The spatial resolution of the radar rainfall composites is 250 meters, and the temporal resolution is 5 minutes. The data from 2013–2014 include measurements from eight radars, the data from 2015 from nine radars, and the data from 2016–2018 from ten radars. The quality of the radar measurements, especially at the edges of the domain, is impacted by the limited coverage of the Finnish radar network. Therefore, in some areas in eastern Finland, the long distances from the closest radar lead to increasing measurement altitudes, which can cause precipitation to be missed or underestimated by the radar. See the detailed description of the radar data in Supplementary Information section C.

Gridded daily precipitation

We used a daily gridded precipitation dataset with a spatial resolution of 1 km from the gridded daily climatology of Finland (Aalto *et al.* 2016; Pirinen *et al.* 2022), which is a part of The Nordic Gridded Climate Dataset (NGCD; Lussana *et al.* (2019)). The gridded data is based on a large array of weather station observations from Finland and neighboring countries, and the geostatistic prediction over a regular 1 km grid resolution is done using kriging interpolation, taking into account elevation, lake and sea coverage, latitude and longitude. The data covers the period from 1961 to the present day, but only the period from 1986 to 2005 is used in this study.

Methods

The analyses presented in this study focus exclusively on Finland's land area (see Supplementary Information Fig. A1). We calculate several statistical metrics, which are summarized in Table 3 and described in more detail below. For hourly scale analyses, we used a 0.1 mm h^{-1} wet hour

Table 3. Statistical indices, and their abbreviations, analyzed in this study.

Abbreviation	Definition	Unit
T	Mean temperature	°C
PrWH	Mean wet hour precipitation intensity	mm h^{-1}
PrMon	Mean monthly precipitation intensity	mm $month^{-1}$
PrD	Mean daily precipitation intensity	mm day^{-1}
PrFreq	Mean frequency of hourly precipitation intensity	count
WHFreq	Mean frequency of wet hours	count
WH	Proportion of wet hours	%
η_a	Apparent hydrological sensitivity	% $°C^{-1}$
Pr95	The mean above the 95th percentile of hourly precipitation intensity	mm h^{-1}
Pr99	The mean above the 99th percentile of hourly precipitation intensity	mm h^{-1}
NPE7	Seasonal mean number of precipitation events exceeding 7 mm h^{-1}	count
NPE20	Seasonal mean number of precipitation events exceeding 20 mm h^{-1}	count
PrWH7	Proportion of wet hours with precipitation ≤ 7 mm h^{-1}	%
PrWH20	Proportion of wet hours with precipitation ≤ 20 mm h^{-1}	%

threshold similarly to Lind *et al.* (2020) and Médus *et al.* (2022). Details of the statistical tests conducted are provided in Supplementary Information section F. We evaluated the HCLIM simulations' accuracy to represent the observed precipitation characteristics in Finland by comparing HCLIM against real-world observational data. We compared the mean wet hour precipitation intensity (PrWH; calculated using the wet hour threshold) from the HCLIM simulations against gauge observations from surface weather stations. A comparison was also conducted for the mean above the 95th and 99th percentile hourly precipitation intensity (using the wet hour threshold to be consistent with observations), and for mean hourly precipitation intensities exceeding 7 mm h^{-1} and 20 mm h^{-1}. For the comparison, HCLIM data was selected from grid boxes containing the coordinates of the surface observation stations or, in some cases near the Finnish border, from the nearest available grid box. The comparison of gauge observations and the HCLIM simulations was done primarily for June–September (JJAS); however, due to the shortage of hourly gauge observations before the year 2010, the comparison was partly extended to encompass annual data, providing a more comprehensive dataset. We also compared HCLIM-erai against radar-derived PrWH in JJAS to examine HCLIM's ability to replicate the spatial precipitation patterns in Finland. We note that the comparison is possible only for a 6-year time period between 2013–2018, and due to this limited climatological representation, only a rough comparison of PrWH between the radar observations and HCLIM-erai is possible. The hourly accumulations from the radar data were calculated by summing the composites within each hour. The weather radar observations were further regridded from 250 m to 3 km to align with the model's resolution.

To validate HCLIM's ability to simulate the seasonal variability of precipitation intensity in different regions of Finland, we compared the 30-day running mean of daily precipitation intensity (PrD; without the wet hour threshold), with gridded precipitation data based on observations. The gridded data is available for all seasons, therefore the comparison is made for the whole year. The comparison was made separately for all the 19 regions in Finland. For simplicity, we focused mainly on four regions at different latitudes.

After the model evaluation analyses, we analyzed the modeled future changes in JJAS precipitation characteristics in Finland by comparing HCLIM-ece and HCLIM-gfdl baseline precipitation characteristics in 1986–2005 to those in the mid-century and late century time periods. In addition to PrWH, for each time period and HCLIM simulation, we calculated Finland's mean temperature (T) and mean monthly precipitation intensity (PrMon; without the wet hour threshold), as well as the apparent hydrological sensitivity as in percentage changes of mean monthly precipitation per Celsius degree (η_a). We expressed the modeled future changes of PrMon and PrWH as ratios and presented them as spatial distributions. To determine the grid cells with statistically significant changes, we conducted a *t*-test. We assessed the significance of these trends using the False Discovery Rate test as outlined by Wilks (2016).

Furthermore, we analyzed how the changes in precipitation occur across different precipitation intensities by dividing the hourly precipitation intensities in HCLIM-ece and HCLIM-gfdl to specific intensity categories and by calculating the mean frequency of precipitation intensity (PrFreq) for each category in each time period. For each category, we calculated the relative change between the baseline and the future periods to assess how the PrFreq distributions shift over time. The mean frequencies are calculated as interannual means, representing the average values across the analyzed 20-year periods. The intensity categories were defined based on the classifications provided by FMI, wherein heavy rain is identified at a threshold of 7 mm h^{-1}, and the national alert level for potentially dangerous rainfall is set at 20 mm h^{-1}. Light rain was divided into categories 0.1–1 mm $h^{-1}$and 1–2 mm h^{-1}, moderate rain into 2–5 mm $h^{-1}$and 5–7 mm h^{-1}, and heavy rain into 7–10 mm h^{-1}, 10–20 mm h^{-1}, and $\geq$ 20 mm h^{-1}. To quantify wet hours, we analyzed the mean frequency of wet hours (WHFreq) for both HCLIM simulations and determined the proportion of wet hours (WH) relative to all hours.

Finally, we conducted a more detailed analysis of the projected changes in short-duration,

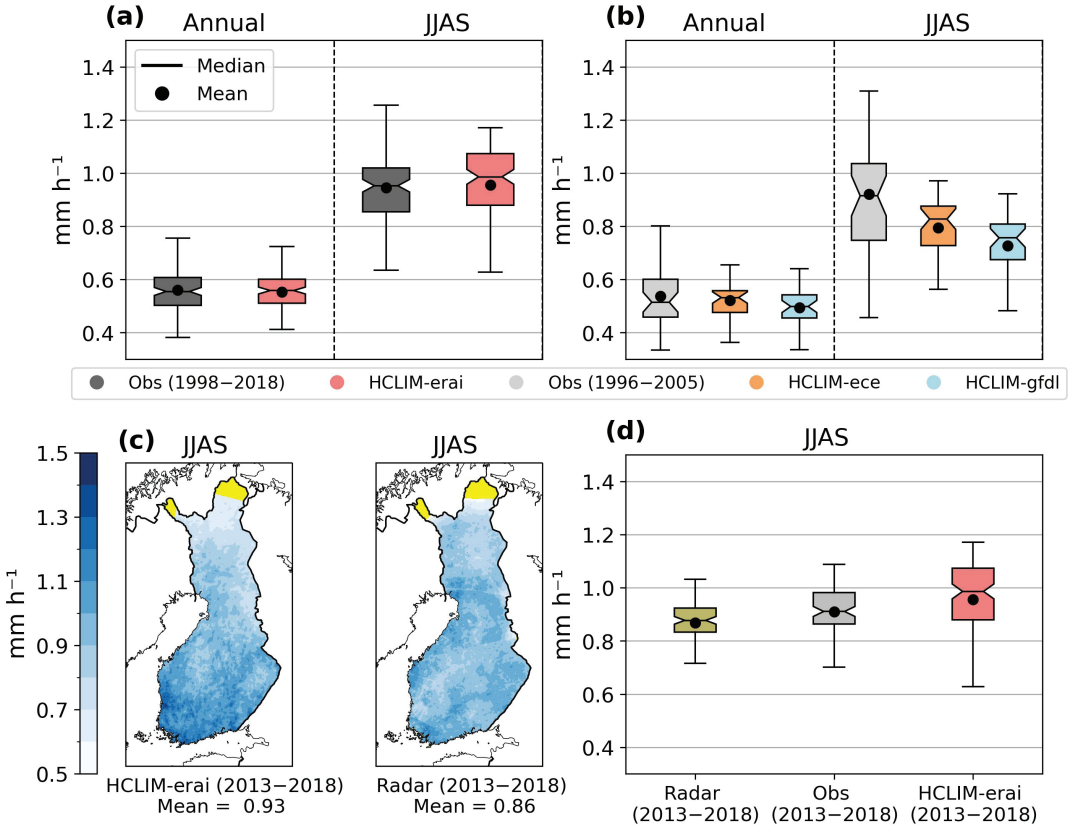

Fig. 1. Comparison of mean wet hour precipitation intensity (PrWH) between the HCLIM simulations and observational datasets in Finland. (**a**) JJAS and annual PrWH in gauge observations (grey) and HCLIM-erai in 1998–2018 (red). (**b**) As in (**a**), but for HCLIM-ece (orange) and HCLIM-gfdl (blue) in 1996–2005. (**c**) Spatial distribution of PrWH in JJAS in 2013–2018 in HCLIM-erai (left) and radar observations (right). The yellow areas indicate regions beyond Finnish radar coverage. (**d**) PrWH in HCLIM-erai (red), gauge observations (grey), and radar observations (green) in JJAS 2013–2018. In (**a**–**b**) and (**d**), HCLIM-erai, HCLIM-ece, HCLIM-gfdl, and radar data are selected from grid points closest to the gauge observation stations. The extent of the boxplots represents the variability of PrWH within Finland. The median of the distribution is represented by the horizontal line whereas the mean is shown by the black dot. The upper and lower horizontal lines show the 75th and 25th percentile and the whiskers extend to data points within a range of 1.5 times the interquartile range (IQR) from the quartiles. In (**c**), radar data is regridded into 3 km resolution.

extreme precipitation events. We investigated the mean above the 95th and 99th percentile (denoted by Pr95 and Pr99, respectively) in each HCLIM simulation in JJAS. We did not use the wet hour threshold for Pr95 and Pr99 as recommended by Schär *et al.* (2016). We also calculated the seasonal mean number of precipitation events exceeding 7 mm h^{-1} (NPE7) and 20 mm h^{-1} (NPE20), and assessed the proportion of hours with precipitation intensities exceeding 7 mm h^{-1} (PrWH7) and 20 mm h^{-1} (PrWH20) relative to the frequency of wet hours (WHFreq) in JJAS.

Results

Evaluation of modeled precipitation

In-situ gauge observations versus HCLIM

We compared the HCLIM-erai, HCLIM-ece, and HCLIM-gfdl simulations against *in-situ* rain gauge observations in Fig. 1a and b to see how well the HCLIM simulations represent the general characteristics of PrWH in Finland. Figures 1a and b show that in all HCLIM simulations and gauge observations, the JJAS medi-

ans of PrWH were higher than the median of the whole year. HCLIM simulations' variability, shown by the whiskers, were within the range of values from gauge observations. The 1998–2018 JJAS median of HCLIM-erai was close to that from gauge observations or, specifically, the median of HCLIM-erai was only 3.5% higher (Fig. 1a). The annual median of HCLIM-erai was also close to the median of the gauge observations, the distributions were near symmetrical, and the spatial variability in the precipitation intensity between observations and HCLIM-erai were similar.

Both the 1996–2005 JJAS and annual medians of HCLIM-ece were higher than those of HCLIM-gfdl, with the biggest difference in the JJAS medians (Fig. 1b). This is in contrast to the results for PrWH in the summer months in Lind *et al.* (2023): fig. 10a, which show greater mean precipitation in HCLIM-gfdl than in HCLIM-ece. The difference may stem from several factors: Lind *et al.* (2023) study spans 20 years, compared to only 10 years in our analysis; it covers Fennoscandia, while we focus on Finland; and the analysis period is JJA, in contrast to JJAS in this study. The JJAS medians in HCLIM-ece and HCLIM-gfdl were lower than in the observations by 9% and 17%, respectively, and the spatial variability in both simulations was smaller than in the observations (Fig. 1b). The annual median of HCLIM-ece was slightly higher than in observations, whereas HCLIM-gfdl's median was slightly lower, and the variability in both simulations was smaller than in the observations. Note, however, that the climatology in the parent GCMs used in the HCLIM-ece and HCLIM-gfdl simulations was not nudged, so the simulated years should only represent typical years for the simulated period (Taylor *et al.* 2012).

We also performed a comparative analysis for the mean above the 95th and 99th percentiles (with wet hour threshold), as well as for mean hourly precipitation intensities exceeding 7 mm h^{-1} and exceeding 20 mm h^{-1}, between the gauge observations and the HCLIM simulations (see Supplementary Information Figs. B2–B3). Figures B2 and B3 show quite similar distributions of the mean above the 95th and 99th percentiles, and moderately similar distributions of mean precipitation intensities exceeding 7 and 20 mm h^{-1}, between HCLIM-erai and observations, although differences are seen in the spatial variability of all metrics. HCLIM-ece and HCLIM-gfdl also show somewhat similar distributions of the mean above the percentiles as in observations, but the intensities are lower, which was also the case for PrWH in Fig. 1b. The distributions of mean hourly intensities exceeding 7 and 20 mm h^{-1} also show lower intensities and smaller spatial variability in HCLIM-ece and HCLIM-gfdl than in the observations (see Supplementary Information Fig. B3). While the model simulations show generally good agreement with observations, at least in terms of the mean above the percentiles, the results should be interpreted with caution due to limitations in the gauge observations used (e.g. in the spatial and temporal coverage), which may lack sufficient robustness for sensitive extreme precipitation comparisons. These limitations could introduce uncertainties and biases in the results, especially for high-intensity precipitation events.

A statistical test for the analyses in Fig. 1a–b was conducted using the two-sample Kolmogorov-Smirnov (KS) test to analyze the maximum difference between the cumulative distribution functions of HCLIM and observations. We used a 90% confidence level, and the results indicated no statistically significant differences between the model and *in-situ* observation distributions, with the exception of a significant difference observed between HCLIM-gfdl and the observations in JJAS (see Supplementary Information Table F1).

Weather radar observations versus HCLIM

We compared PrWH of HCLIM-erai against weather radar observations (Fig. 1c). Figure 1c shows that both radar and HCLIM-erai exhibit somewhat similar regional distribution of PrWH in Finland in JJAS, with a spatial Pearson correlation coefficient value of 0.48 (for the fit, see Supplementary Information Fig. F2). Regions like the coast of the Gulf of Bothnia, Finnish Lakeland and southern Finland exhibit higher PrWH values compared to Lapland and the central parts of Finland. HCLIM-erai shows a south-

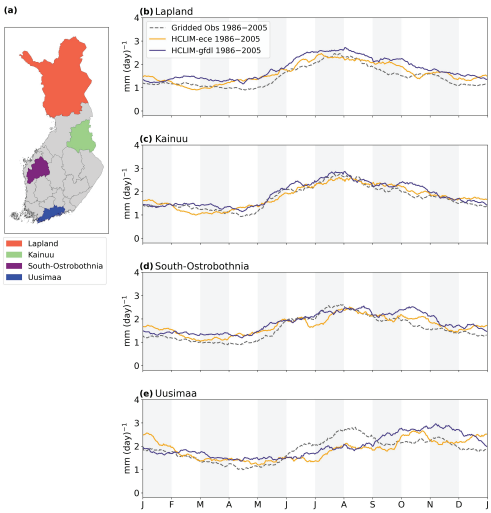

Fig. 2. The annual cycle of the 30 day running mean of daily precipitation (PrD; mm day^{-1}) calculated from the gridded daily precipitation observations (grey dashed line), HCLIM-ece (orange line) and HCLIM-gfdl (blue line) in 1986–2005. The lines represent regional averages over (**a**) four regions in Finland, which are: (**b**) Lapland, (**c**) Kainuu, (**d**) South-Ostrobothnia, and (**e**) Uusimaa.

to-north gradient in PrWH, which is less apparent in radar observations.

Figure 1d shows the distribution of PrWH in HCLIM-erai, gauge observations, and radar observations for the relatively short period of data overlap (2013–2018; JJAS). The median in HCLIM-erai is higher than in both the gauge and radar observations, and the spread is larger. The median of HCLIM-erai is closer to gauge observations than to radar observations, and importantly, the median in radar observations is lower than in the gauge observations. The difference between the gauge and radar distributions likely arises from different measurement methodologies and related uncertainties, which likely impact the PrWH value of radar observations.

Gridded daily precipitation versus HCLIM

Figure 2a presents the running mean of PrD in 1986–2005, calculated from the gridded observational dataset, HCLIM-ece and HCLIM-gfdl, in four regions from different latitudes: Uusimaa in southern Finland (~60°), South-Ostrobothnia in central Finland (~62°), Kainuu in central-to-northern Finland (~64°), and Lapland (above ~66°). The running mean of PrD in those regions resembled those observed in other regions at similar latitudes. The models' PrD aligns closely with the gridded observation data. The annual cycles also agree well across regions except in Uusimaa (Fig. 2e), where the highest precipitation peak occurs later in the models than observed. Neither model significantly outperforms the other in matching with the observations. In Uusimaa, both HCLIM-ece and HCLIM-gfdl show mostly lower PrD values in June, July, and August compared to observations (Fig. 2e). During autumn months (September, October and November), HCLIM-gfdl consistently shows higher PrD values than what is observed for 18 out of 19 regions (see Supplementary Information Fig. E1–E2). In Kainuu and South-Ostrobothnia, models show a high agreement with the observations (Fig. 2c and d). In Lapland, the models show consistently somewhat higher PrD values than what has been observed (Fig. 2b).

Projected future changes in summertime precipitation

We analyzed the modeled future changes in precipitation characteristics in Finland in JJAS by comparing HCLIM-ece and HCLIM-gfdl precipitation characteristics in 1986–2005 to those in mid-century and late century. The evaluation results above indicate that the HCLIM simulations capture the main characteristics of summertime precipitation in Finland well, including the timing of peak precipitation from the annual cycle of mean daily precipitation, which supports the use of the JJAS season for analyzing extreme precipitation. In assessing the ability of HCLIM to represent current climate conditions, these results affirm the suitability of the HCLIM simulations for studies on projected changes in JJAS precipitation. While there are some limitations in robustly analyzing extreme precipitation against *in-situ* observations in Finland, studies by Lind *et al.* (2020) and Médus *et al.* (2022) have demonstrated encouraging extreme precipitation evaluation results for HCLIM simula-

tions in other parts of Fennoscandia, providing a strong basis to assume that the model captures extreme characteristics in Finland as well.

Changes in monthly and wet hour precipitation intensity and in the frequency of wet hours

Relative to the historical period (1986–2005), HCLIM-ece projects a warming of 4.4 °C (JJAS) in Finland in the end of the century under RCP8.5, whereas HCLIM-gfdl projects a greater warming of 7.3 °C (Table 4). In general, CMIP5 models project an ensemble average warming of 4.7 °C in Finland (model spread being 2.5–6.9 °C with a 90% confidence interval; see Ruosteenoja *et al.* 2016) between 1981–2010 and 2070–2099 in the RCP8.5 scenario. We calculated η_a for the future periods and observed that HCLIM-gfdl projects higher η_a values compared to HCLIM-ece, which shows both positive and negative η_a values depending on the time period (Table 1). We note that both HCLIM-ece and HCLIM-gfdl are markedly cold-biased relative to gridded observational daily temperature data, while PrMon in those simulations agrees rather well with observations.

In Finland in JJAS, PrMon is projected to increase by late century in HCLIM-ece RCP4.5 and RCP8.5 scenarios, as well as in the HCLIM-gfdl RCP8.5 scenario, as shown in Table 4. However, the changes of PrMon differ in sign between HCLIM-ece and HCLIM-gfdl, with HCLIM-ece showing slightly negative changes in some regions and HCLIM-gfdl showing only positive changes (Fig. 3a–b). By mid-century (Fig. 3a), HCLIM-ece projects an increase in PrMon in southern Finland and northernmost Lapland, while other regions exhibit a decrease or no change. In contrast, HCLIM-gfdl shows an increase in PrMon across the country, and the change has a notable south-to-north gradient, with the magnitude being higher in the south and decreasing towards the north. By late century (Fig. 3b), both HCLIM-ece and HCLIM-gfdl project a relatively homogeneous increase (no clear south-to-north gradient) across the country, and the increase is stronger in HCLIM-gfdl than in HCLIM-ece (17% and 7%, respectively) in the RCP8.5 scenario (Table 4). These differences again highlight the sensitivity of the HCLIM simulations to the parent GCM applied for the boundary conditions.

The changes in PrWH (Fig. 3c–d, Table 4) are positive across the country in all simulations. The spatial distribution of the change somewhat differs between HCLIM-ece and HCLIM-gfdl. The spatial distribution of the change in PrWH also differs from that of the PrMon (Fig. 3a–b).

Table 4. The changes in temperature (ΔT), mean monthly precipitation intensity (ΔPrMon), and mean wet hour precipitation intensity (ΔPrWH) in Finland in JJAS between the future and historical periods, shown for HCLIM-ece and HCLIM-gfdl and the different RCP scenarios. Additionally, the proportion of wet hours (WH) in all time periods, and its relative change with respect to the historical period (denoted as RC(WH)), are shown in percentages.

Dataset and period	Scenario	ΔT (°C)	ΔPrMon (%; monthly)	ΔPrWH (%; hourly)	WH (%)	RC(WH) (Δ%)
HCLIM-ece						
1986—2005	historical				11.0	
2041—2060	RCP4.5	1.6	—3	7	9.9	—8
	RCP8.5	2.4	—0	19	9.1	—16
2081—2100	RCP4.5	2.3	4	16	9.6	—11
	RCP8.5	4.4	7	32	8.9	—18
HCLIM-gfdl						
1986—2005	historical				12.8	
2041—2060	RCP8.5	4.0	14	31	11.3	—12
2081—2100	RCP8.5	7.3	17	63	9.6	—25

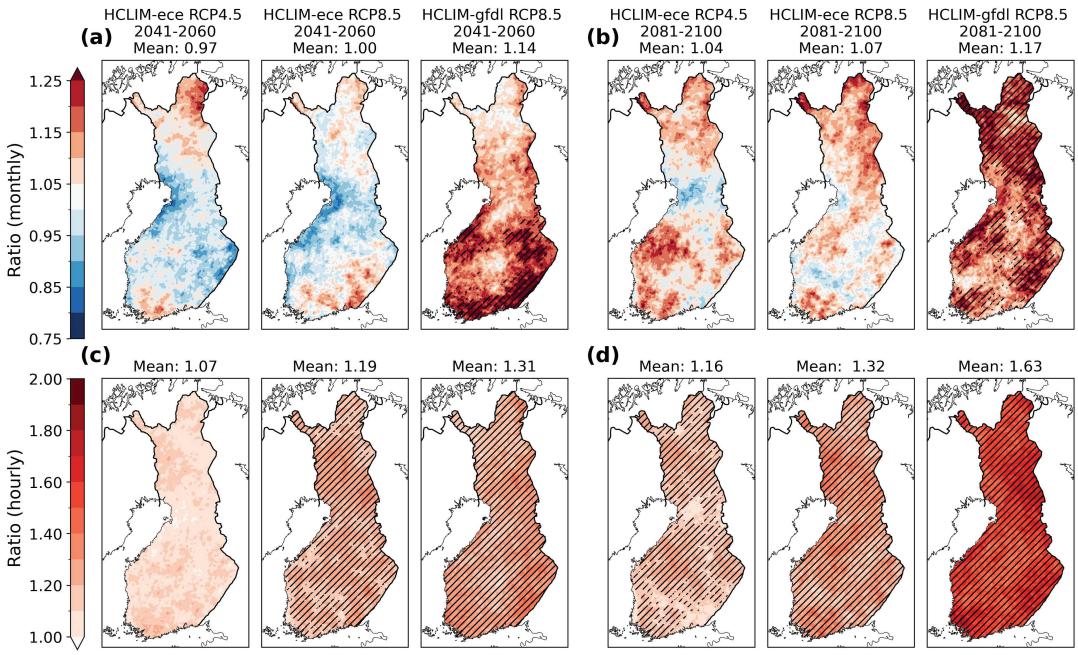

Fig. 3. (**a**) The mean monthly precipitation intensity (PrMon) change in JJAS in HCLIM-ece RCP4.5 (left), HCLIM-ece RCP8.5 (center), and HCLIM-gfdl RCP8.5 (right) by mid-century, and (**b**) same as in (**a**) by late century. (**c**) The mean wet hour precipitation intensity (PrWH) change for the same simulations as in (a) by mid-century, and (d) by late century. The changes are with respect to the historical period. The wet hour threshold of 0.1 mm h^{-1} is used in (**c**) and (**d**), whereas the monthly means in (**a**) and (**b**) are calculated without the wet hour threshold. The hatched patterns indicate areas with statistically significant differences between the historical simulation and future projections.

Mean increase in PrWH, averaged over Finland, ranges from 7% to 31% by mid-century (Fig. 3c), and from 16% to 63% by late century (Fig. 3d), with HCLIM-gfdl again projecting generally larger changes than HCLIM-ece.

A factor of the difference between the changes in PrMon and PrWH may be explained by a rather large projected change in WHFreq. When all grid points in the Finnish land area are considered, WH is 11% during the historical period 1986–2005 according to HCLIM-ece and 13% according to HCLIM-gfdl (Fig. 4, Table 4). Both simulations project a decrease in WHFreq by one to two percentage points leading WH to decrease down to 9–11% by mid-century, and even further to 9% for all the simulations by late century. WH decreases from the historical period by 8–16% by mid-century in both HCLIM-ece and HCLIM-gfdl. By late-century, the decrease is 11% (RCP4.5) and 18% (RCP8.5) in HCLIM-ece, and 25% (RCP8.5) in HCLIM-gfdl. While WHFreq is higher in HCLIM-gfdl than in HCLIM-ece in the historical period, this difference diminishes in the late century simulations. The RCP8.5 scenario shows statistically significant differences in the distributions, suggesting significant changes in WHFreq compared to the historical period. In contrast, the RCP4.5 scenario shows no significant differences, indicating closer alignment with the historical simulation (see Table F2 in Supplementary Information).

Changes in hourly precipitation intensity categories

We analyzed the relative changes in PrFreq of different intensity categories between the historical period and the future simulations (Fig. 5). Our categorization reveals that low-intensity events occur more frequently than high-intensity ones (Fig. 5a). The relative changes in PrFreq, shown in Fig. 5b, are mostly negative for low intensity categories (0.1–2 mm h^{-1}). The relative change is positive for the higher intensity categories (≥ 2 mm h^{-1}), and the magnitude

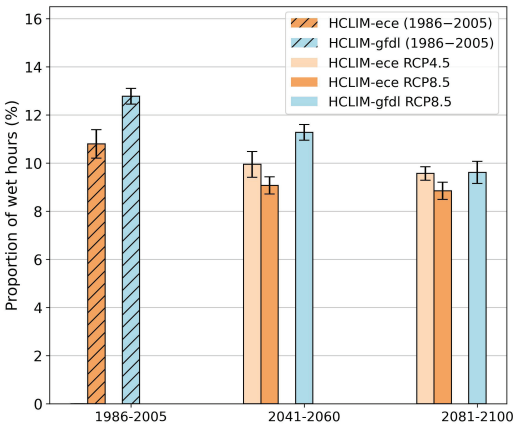

Fig. 4. The proportion of wet hours to all hours (WH) in the historical and the future periods in Finland in JJAS. WH is shown for the RCP4.5 and RCP8.5 scenarios in HCLIM-ece, and for RCP8.5 in HCLIM-gfdl. The error bars represent the standard error of interannual means.

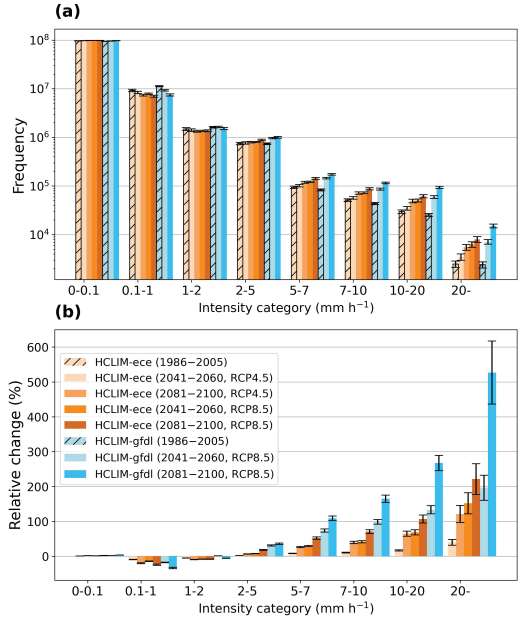

Fig. 5. (**a**) The mean frequency of hourly precipitation intensity (PrFreq) in the specified intensity categories for HCLIM-ece and HCLIM-gfdl in Finland in JJAS, and (**b**) the relative change of PrFreq between the historical period and the future periods. The error bars represent the standard error of the interannual mean.

of the positive change becomes greater with higher intensity categories. The magnitudes of the relative changes in HCLIM-gfdl are again larger than those in HCLIM-ece, and the relative changes are larger under the RCP8.5 scenario compared to RCP4.5.

We calculated how NPE7 (i.e. number of heavy rain events) and NPE20 (i.e. number of events exceeding the first warning limit of short duration rain potentially causing flooding) will change in Finland (Table 5). In the RCP8.5 scenario, NPE7 becomes 1.5 (2.1) times as common by mid-century compared to the historical period and 1.9 (3.1) as common by late century in HCLIM-ece (HCLIM-gfdl). In the RCP4.5 scenario simulated by HCLIM-ece, the changes remain more modest: NPE7 become 1.1 times as common by mid-century

Table 5. The seasonal mean number of precipitation events exceeding 7 mm h^{-1} (NPE7) and 20 mm h^{-1} (NPE20) in Finland in JJAS in the different periods, and the ratio between the values in the future and historical periods, in HCLIM-ece and HCLIM-gfdl and the different RCP scenarios.

Dataset and period	Scenario	NPE7	Ratio	NPE20	Ratio
HCLIM-ece					
1986—2005	historical	83 852		2497	
2041—2060	RCP4.5	95 214	1.1	3495	1.4
	RCP8.5	126 471	1.5	5521	2.2
2081—2100	RCP4.5	129 456	1.5	6291	2.5
	RCP8.5	157 675	1.9	8024	3.2
HCLIM-gfdl					
1986—2005	historical	71 566		2408	
2041—2060	RCP8.5	153 320	2.1	7142	3.0
2081—2100	RCP8.5	224 381	3.1	15 096	6.0

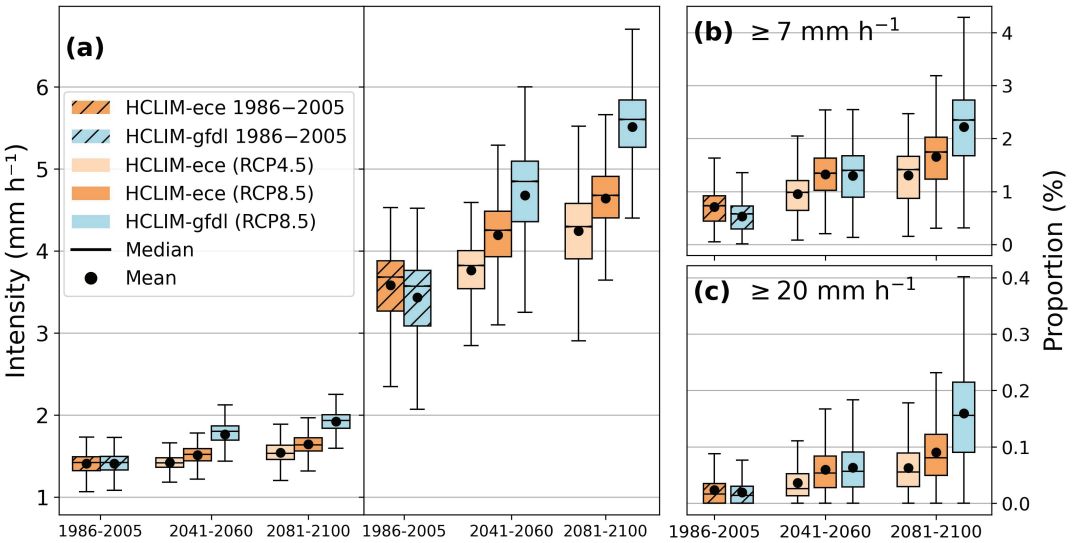

Fig. 6. (**a**) The mean above the 95th percentile (Pr95; left in (**a**)) and the mean above the 99th percentile (Pr99; right in (**a**)) of hourly precipitation intensity in Finland in JJAS in the different time periods in HCLIM-ece and HCLIM-gfdl. (**b**) The proportion of wet hours with precipitation intensities exceeding (**b**) 7 mm h^{-1} (PrWH7) and (**c**) 20 mm h^{-1} (PrWH20) relative to the frequency of wet hours (WHFreq) in JJAS. See Fig. 1 for the details regarding the boxplots.

and 1.5 times as common by late century. For NPE20, the changes are considerably stronger: in RCP8.5 scenario, the events are projected to become 2.2 (3.0) as common by mid-century and 3.2 (6.0) times as common by late century. In the RCP4.5 scenario in HCLIM-ece, NPE20 become 1.4 times as common by mid-century and 2.5 times as common by late century.

The changes in strong or extreme short-duration precipitation in Finland are further presented in Fig. 6. The median of Pr95 increases in both HCLIM-ece and HCLIM-gfdl by the late century (Fig. 6a) by 8% in HCLIM-ece (RCP4.5), 15% in HCLIM-ece (RCP8.5), and 36% in HCLIM-gfdl (RCP8.5). Again, the increase is greater under RCP8.5 than RCP4.5, and the change is stronger in HCLIM-gfdl. The increase is even stronger for the median of Pr99, ranging from 17% in HCLIM-ece (RCP4.5) to 57% in HCLIM-gfdl (RCP8.5) by the century's end. Additionally, PrWH7 and PrWH20 also are projected to change (Fig.. 6b and c). Both PrWH7 and PrWH20 increase in HCLIM-ece and HCLIM-gfdl already by mid-century and the increase persists by the end of the century. This can be explained partly by the decrease in WHFreq (Fig. 4), but mainly by the increase in higher intensity categories of PrFreq (Fig. 5b). Consistent with prior results, the change is more rapid in HCLIM-gfdl than in HCLIM-ece. Moreover, the spatial variability in Finland increases more in HCLIM-gfdl than in HCLIM-ece in late century.

Discussion and conclusions

Since the 1990s, GCMs have projected the annual precipitation in Finland to increase as the global warming proceeds (Carter *et al.* 1996; Ruosteenoja *et al.* 2021). However, it is well known that even modern-day GCMs tend to "drizzle" — generating too frequent and long-duration precipitation at too low intensity (see e.g. Chen *et al.* (2021)). Additionally, certain key atmospheric processes, such as deep convection, are not explicitly resolved in these coarse-resolution GCMs but are instead approximated through parameterizations. These undermine our ability to analyze projected changes in regional precipitation intensity using GCM data alone. To overcome this problem, GCM projections can be downscaled to convection-permitting resolution (e.g. Arakawa *et al.* (2013)).

Here, we have analyzed convection-permitting regional climate model projections from HCLIM (run with the HCLIM38-AROME configuration) generated in the NorCP project (Lind *et al.* 2020), where projections from two CMIP5-era parent GCMs, EC-Earth2 and GFDL-CM3, were downscaled with a double-nested approach to 3 km resolution over Fennoscandia. The parent GCMs used as HCLIM boundary conditions differed greatly in their future climate change signals: GFDL-CM3 exhibits rapid warming at high latitudes, while EC-Earth2 projects milder warming that aligns with the CMIP5 average (Lind *et al.* 2023).

The analysis included a historical 20-year period (1986–2005) and two future 20-year intervals: mid-century (2041–2060) and late century (2081–2100). The analyzed future projections used downscaled EC-Earth2 and GFDL-CM3 model data under two emission scenarios, RCP4.5 (EC-Earth only) and RCP8.5. While RCP8.5 represents an unlikely outcome compared to RCP4.5, it serves as an upper bound for exploring potential precipitation changes. At mid-century, a critical timeframe for many stakeholders, the differences between RCP4.5 and RCP8.5 remain relatively small. Including both scenarios allows us to capture a range of possible outcomes, providing valuable insights for understanding changes and developing robust policies while addressing uncertainties in future projections.

First, we analyzed summertime (JJAS) precipitation characteristics in Finland, generated by HCLIM, by comparing the historical period model data against a set of observations, extending the model data evaluation presented in Médus *et al.* (2022). Overall, HCLIM-ece and HCLIM-gfdl were found to be cold-biased in temperature. Nevertheless, both were in a relatively good correspondence with observations in their precipitation characteristics both at monthly and hourly timescales, specifically in terms of the mean monthly precipitation intensity (PrMon) and mean wet hour precipitation intensity (PrWH), and their variability within Finland. The timing of the peak in the annual cycle of mean daily precipitation intensity (PrD) supported the use of the JJAS season for analyzing extreme precipitation.

The simulated future changes in precipitation were found to be sensitive to the applied GCM used as HCLIM boundary condition, as perhaps expected. Notably, the changes in PrMon by mid-century in JJAS varied both in magnitude and direction between HCLIM-ece and HCLIM-gfdl, while both models did project an overall PrMon increase by late century. In RCP8.5 simulations by late century, the apparent hydrological sensitivity (η_a) was found to be 1.5–1.8% $^{o}C^{-1}$ (HCLIM-ece) and 2.4% $^{o}C^{-1}$ (HCLIM-gfdl) in JJAS, while the CMIP6 model ensemble projects η_a to be 0.9–2.1% $^{o}C^{-1}$ in SSP5-8.5 in summer (JJA) in Finland (Ruosteenoja *et al.* (2021), fig. 7, tables S1 and S2).

Notably, both simulations also agreed on the sign of change in PrWH and the decreasing trend in the mean frequency of wet hours (WHFreq). The proportion of wet hours (WH), which was calculated from the whole area of Finland, decreased from 11–13% to 9–11% by mid-century, and further reducing to around 9% across all simulations and scenarios by late century. High-intensity PrFreq becomes more common compared to the historical period in all simulations. According to the simulations, climate change intensifies PrFreq exceeding ≥ 2 mm h^{-1}, and the changes become greater for the categories of higher intensities.

Of particular interest are the projected changes in the intensity categories used in the alert classification made by FMI, wherein heavy rain is identified at a threshold of 7 mm h^{-1}, and the national alert level for potentially dangerous rainfall is set at 20 mm h^{-1}. According to the simulations, both the seasonal mean number of precipitation events exceeding 7 mm h^{-1} (NPE7) and 20 mm h^{-1} (NPE20) in Finland will increase greatly as the climate change proceeds. Already by mid-century in RCP8.5, NPE7 will become 1.5 (2.1) times as common as in the historical period. By the late century, NPE7 are projected to become 1.9 (3.1) times as common. In RCP4.5 scenario, the increases are more modest, changing by factors of 1.1 by mid-century and 1.5 by late century. For the more severe events (NPE20), the change is considerably higher; by mid-century in RCP8.5, increasing by factors of 2.2 (3.0) in HCLIM-ece (HCLIM-gfdl), and by late century, by factors of 3.2 (6.0).

Additionally, when considering the proportion of wet hours with precipitation exceeding 7 mm h^{-1} (PrWH7) and 20 mm h^{-1} (PrWH20), we see a change in their contribution to overall wet hours. By mid-century in RCP8.5, PrWH7 will increase to 1.3% (1.4%) in HCLIM-ece (HCLIM-gfdl), up from the historical period's proportion of 0.7% (0.6%). By the late century, these events are projected to rise further to 1.7% (2.4%). In RCP4.5 scenario, the increases are more modest, PrWH7 rising to 1.0% by mid-century and 1.4% by late century. For the more severe PrWH20, by mid-century, the median proportion is expected to increase to 0.05% (0.06%) in HCLIM-ece (HCLIM-gfdl), and by late century, to 0.08% (0.16%).

We note that our analysis is based only on a small ensemble of downscaled simulations (three periods with two GCMs and two scenarios), limited by the high computational cost of convection-permitting HCLIM runs. The analyzed 20-year time slices are, individually, rather short for studying climatological averages for Finland, where the natural variability of summer climate conditions is relatively high. However, analyzing two scenarios, two timeframes, and two parent GCMs allows us to explore a range of possible outcomes while addressing uncertainties in future projections. Yet, expanding the GCM ensemble size and extending simulation durations would enhance the robustness of the results for a given emission pathway. Alternative approaches, such as the pseudo-global-warming method (e.g. Brogli *et al.* (2023)), in which reanalysis data is downscaled for different climate states using GCM output, may provide valuable new avenues for downscaling regional climate change signals at a high signal-to-noise ratio compared to computational cost.

The increase in the frequency of heavy and extreme precipitation events shown in this study can thus represent a serious hazard in Finland for various sectors. In agriculture, this trend is likely to worsen crop damage, jeopardizing food security and farmer livelihoods. Urban areas face heightened risks of flash floods, which can disrupt daily life, damage infrastructure, and increase maintenance costs. The transportation sector is also vulnerable, as heavy rains can weaken road safety and efficiency, leading to increased accidents and traffic delays. Consequently, enhancing preparedness and responsiveness for these heavy precipitation events are one of the crucial regional adaptation strategies to climate change. This involves comprehensive planning in sectors such as urban development, transportation, and agriculture to mitigate risks and safeguard communities against the escalating impacts of extreme weather.

Acknowledgements: The HCLIM data used in this study has been produced by the NorCP project, which is a Nordic collaboration involving climate modeling groups from the Danish Meteorological Institute (DMI), Finnish Meteorological Institute (FMI), Norwegian Meteorological Institute (MET Norway) and the Swedish Meteorological and Hydrological Institute (SMHI). This study was funded by the FINSCAPES project (Finnish Scenarios for Climate Change Research Addressing Policies, Regions and Integrated Systems; Grant Number 342561, Research Council of Finland's call 'Special funding for system-level research into climate change mitigation and adaptation'), by Research Council of Finland's Atmosphere and Climate Competence Center (ACCC) Flagship program, Grant Numbers 337552 and 357904 and by the European Union project PIISA (Piloting Innovative Insurance Solutions for Adaptation; Grant Number 101112841). We also wish to acknowledge Ari Aaltonen's (FMI) and Maria Santanen's (FMI) help in accessing the observational hourly precipitation data.

Data availability: Hourly gauge observations were obtained from the Finnish Meteorological Institute's Open Data -service (https://en.ilmatieteenlaitos.fi/open-data). The gridded dataset used is a sub-set of the NGCD product (CDS 2021). The NorCP data is accessible upon request and the gauge-corrected weather radar data is available upon request from the authors.

Supplementary Information: This paper is accompanied by a supplementary file, which provides additional details and visualizations to support the main findings. The contents of the supplementary file are as follows: (A) HCLIM domain and its orography over Fennoscandia; (B) In-situ gauge extreme observations versus HCLIM; (C) description of radar data; (D) All spatial distributions of HCLIM simulations in Finland; (E) Gridded daily precipitation versus HCLIM 30-day running mean time-series for all regions in Finland; and (F) Additional statistical analyses that provide further insights into the study's results. The supplementary information related to this article is available online at: http://hdl.handle.net/10138/594852

References

Aalto, J., Pirinen, P., and Jylhä, K. 2016. New gridded daily climatology of Finland: Permutation-based uncertainty estimates and temporal trends in climate. Journal of Geophysical Research: Atmospheres. 121: 3807–3823.

Arakawa, A. and Wu, C.-M. 2013. A unified representation of deep moist convection in numerical modeling of the

atmosphere. Part I. Journal of the Atmospheric Sciences. 70: 1977–1992.

Bednar-Friedl, B., Biesbroek, R., Schmidt, D. N., Alexander, P., Børsheim, K. Y., Carnicer, J.,Georgopoulou, E., Haasnoot, M., Le Cozannet, G., Lionello, P., Lipka, O., Möllmann, C., Muccione, V., Mustonen, T., Piepenburg, D., and Whitmarsh, L. 2022. Europe. In: Climate Change 2022: Impacts, Adaptation and Vulnerability. Contribution of Working Group II to the Sixth Assessment Report of the Intergovernmental Panel on Climate Change. Cambridge University Press, Cambridge, UK and New York, NY, USA: 1817–1927. doi: 10.1017/9781009325844.015.

Belusić, D., de Vries, H., Dobler, A., Landgren, O., Lind, P., Lindstedt, D., Pedersen, R. A., Sánchez-Perrino, J. C., Toivonen, E., van Ulft, B., Wang, F., Andrae, U., Batrak, Y., Kjellström, E., Lenderink, G., Nikulin, G., Pietikäinen, J.-P., Rodríguez-Camino, E., Samuelsson, P., van Meijgaard, E., and Wu, M. 2020. HCLIM38: a flexible regional climate model applicable for different climate zones from coarse to convection-permitting scales. Geoscientific Model Development. 13: 1311–1333.

Brogli, R., Heim, C., Mensch, J., Sørland, S. L., and Schär, C. 2023. The pseudo-global-warming (PGW) approach: methodology, software package PGW4ERA5 v1.1, validation, and sensitivity analyses. Geoscientific Model Development. 16: 907–926. doi: 10.5194/gmd-16-907-2023.

Carter, T., Posch, M., and Tuomenvirta, H. 1996. The SILMU scenarios: specifying Finland's future climate for use in impact assessment. Geophysica. 32: 235–260.

CDS. 2021. Nordic gridded temperature and precipitation data from 1971 to present derived from in-situ observations. Copernicus Climate Change Service (C3S) Climate Data Store (CDS). Last accessed: 2025-01-15. doi: 10.24381/cds.e8f4a10c.

Chen, D., Dai, A., and Hall, A. 2021. The convective-to-total precipitation ratio and the "drizzling" bias in climate models. Journal of Geophysical Research: Atmospheres. 126:E2020JD034198.

Christensen, O. B., Kjellström, E., Dieterich, C., Gröger, M., and Meier, H. E. M. 2022. Atmospheric regional climate projections for the Baltic Sea region until 2100. Earth System Dynamics. 13: 133–157.

Climate Change (IPCC), I. P. on. 2023. "Climate Change Information for Regional Impact and for Risk Assessment". Climate Change 2021 – The Physical Science Basis: Working Group I Contribution to the Sixth Assessment Report of the Intergovernmental Panel on Climate Change. Cambridge University Press: 1767–1926.

Dee, D. P., Uppala, S. M., Simmons, A. J., Berrisford, P., Poli, P., Kobayashi, S., Andrae, U., Balmaseda, M., Balsamo, G., Bauer, d. P., *et al.* 2011. The ERA-Interim reanalysis: Configuration and performance of the data assimilation system. Quarterly Journal of the Royal Meteorological Society. 137: 553–597.

Donner, L. J., Wyman, B. L., Hemler, R. S., Horowitz, L. W., Ming, Y., Zhao, M., Golaz, J.-C., Ginoux, P., Lin, S.-J., Schwarzkopf, M. D., *et al.* 2011. The dynamical core, physical parameterizations, and basic simulation characteristics of the atmospheric component AM3 of the GFDL global coupled model CM3. Journal of Climate. 24: 3484–3519.

Douville, H., Raghavan, K., Renwick, J., Allan, R. P., Arias, P. A., Barlow, M., Cerezo-Mota, R., Cherchi, A., Gan, T. Y., Gergis, J., Jiang, D., Khan, A., Pokam Mba, W., Rosenfeld, D., Tierney, J., and Zolina, O. 2021. Water Cycle Changes. In Climate Change 2021: The Physical Science Basis. Contribution of Working Group I to the Sixth Assessment Report of the Intergovernmental Panel on Climate Change. Cambridge University Press, Cambridge, United Kingdom and New York, NY, USA: 1055–1210. doi: 10.1017/9781009157896.010.

Dyrrdal, A. V., Olsson, J., Médus, E., Arnbjerg-Nielsen, K., Post, P., Aniskevica, S., Thorn-dahl, S., Førland, E., Wern, L., Maciulyté, V., and Mäkelä, A. 2021. Observed changes in heavy daily precipitation over the Nordic-Baltic region. Journal of Hydrology: Regional Studies. 38: 100965.

Emanuel, K. A. 1994. Atmospheric convection. Oxford University Press, USA.

Fischer, E. M. and Knutti, R. 2014. Detection of spatially aggregated changes in temperature and precipitation extremes. Geophysical Research Letters. 41: 547–554.

FMI: Heavy Rain Warning, n.d. Warnings about rains causing flooding. Finnish Meteorological Institute (FMI). https://en.ilmatieteenlaitos.fi/heavy-rain-warning. Last accessed: 2025-01-15.

Hazeleger, W., Severijns, C., Semmler, T., Stefanescu, S., Yang, S., Wang, X., Wyser, K., Dutra, E., Baldasano, J. M., Bintanja, R., *et al.* 2010. EC-Earth: a seamless earth-system prediction approach in action. Bulletin of the American Meteorological Society. 91: 1357–1364.

Irannezhad, M., Chen, D., Kløve, B., and Moradkhani, H. 2017. Analysing the variability and trends of precipitation extremes in Finland and their connection to atmospheric circulation patterns. International Journal of Climatology. 37: 1053–1066.

Kendon, E. J., Roberts, N. M., Senior, C. A., and Roberts, M. J. 2012. Realism of rainfall in a very high-resolution regional climate model. American Meteorological Society. 25: 5791–5806.

Lehtonen, I. and Jylhä, K. 2019. Tendency towards a more extreme precipitation climate in the Coupled Model Intercomparison Project Phase 5 models. Atmospheric Science Letters. 20: e895.

Lehtonen, I., Ruosteenoja, K., and Jylhä, K. 2014. Projected changes in European extreme precipitation indices on the basis of global and regional climate model ensembles. International journal of climatology. 34.

Lind, P., Belusić, D., Christensen, O. B., Dobler, A., Kjellström, E., Landgren, O., Lindstedt, D., Matte, D., Pedersen, R. A., Toivonen, E., *et al.* 2020. Benefits and added value of convection-permitting climate modeling over Fenno-Scandinavia. Climate Dynamics. 55: 1893–1912.

Lind, P., Belusić, D., Médus, E., Dobler, A., Pedersen, R. A., Wang, F., Matte, D., Kjellström, E., Landgren, O., Lindstedt, D., *et al.* 2023. Climate change information over

Fenno-Scandinavia produced with a convection-permitting climate model. Climate Dynamics. 61: 519–541.

Lucas-Picher, P., Argüeso, D., Brisson, E., Tramblay, Y., Berg, P., Lemonsu, A., Kotlarski, S., and Caillaud, C. 2021. Convection-permitting modeling with regional climate models: Latest developments and next steps. Wiley Interdisciplinary Reviews: Climate Change. 12:e731.

Lussana, C., Tveito, O. E., Dobler, A., and Tunheim, K. 2019. seNorge 2018, daily precipitation, and temperature datasets over Norway. Earth System Science Data. 11: 1531–1551.

Madsen, H. M., Andersen, M. M., Rygaard, M., and Mikkelsen, P. S. 2018. Definitions of event magnitudes, spatial scales, and goals for climate change adaptation and their importance for innovation and implementation. Water research. 144: 192–203.

Médus, E., Thomassen, E. D., Belusić, D., Lind, P., Berg, P., Christensen, J. H., Christensen, O. B., Dobler, A., Kjellström, E., Olsson, J., *et al.* 2022. Characteristics of precipitation extremes over the Nordic region: added value of convection-permitting modeling. Natural hazards and earth system sciences. 22: 693–711.

Mironov, D., Heise, E., Kourzeneva, E., Ritter, B., Schneider, N., and Terzhevik, A. 2010. Implementation of the lake parameterisation scheme FLake into the numerical weather prediction model COSMO. Boreal Environ. Res. 15: 218–230

Moss, R. H., Edmonds, J. A., Hibbard, K. A., Manning, M. R., Rose, S. K., Van Vuuren, D. P., Carter, T. R., Emori, S., Kainuma, M., Kram, T., *et al.* 2010. The next generation of scenarios for climate change research and assessment. Nature. 463: 747–756.

Myhre, G., Alterskjær, K., Stjern, C. W., Hodnebrog, Ø., Marelle, L., Samset, B. H., Sillmann, J., Schaller, N., Fischer, E., Schulz, M., *et al.* 2019. Frequency of extreme precipitation increases extensively with event rareness under global warming. Scientific reports. 9: 16063.

Olsson, J., Dyrrdal, A. V., Médus, E., Södling, J., Aniskevica, S., Arnbjerg-Nielsen, K., Førland, E., Maciulyt˙e, V., Mäkelä, A., Post, P., *et al.* 2022. Sub-daily rainfall extremes in the Nordic–Baltic region. Hydrology Research. 53: 807–824.

Pedretti, D. and Irannezhad, M. 2019. Non-stationary peaks-over-threshold analysis of extreme precipitation events in Finland, 1961–2016. International Journal of Climatology. 39: 1128–1143.

Pirinen, P., Lehtonen, I., Heikkinen, R. K., Aapala, K., and Aalto, J. 2022. Daily gridded evapotranspiration data for Finland for 1981–2020. FMI's Climate Bulletin Research Letters. 4: 35–37.

Prein, A. F., Langhans, W., Fosser, G., Ferrone, A., Ban, N., Goergen, K., Keller, M., Tölle, M., Gutjahr, O., Feser, F., Brisson, E., Kollet, S., Schmidli, J., Lipzig, N. P. M. van, and Leung, R. 2015. A review on regional convection-permitting climate modeling: Demonstrations, prospects, and challenges. Reviews of Geophysics. 53: 323–361.

Ruosteenoja, K. and Jylhä, K. 2021. Projected climate change in Finland during the 21st century calculated from CMIP6 model simulations. Geophysica. 56: 39–69.

Ruosteenoja, K., Jylhä, K., and Kämäräinen, M. 2016. Climate projections for Finland under the RCP forcing scenarios. Geophysica. 51.

Rutgersson, A., Kjellström, E., Haapala, J., Stendel, M., Danilovich, I., Drews, M., Jylhä, K., Kujala, P., Larsén, X. G., Halsnæs, K., Lehtonen, I., Luomaranta, A., Nilsson, E., Olsson, T., Särkkä, J., Tuomi, L., and Wasmund, N. 2022. Natural hazards and extreme events in the Baltic Sea region. Earth System Dynamics. 13: 251–301.

Saltikoff, E., Huuskonen, A., Hohti, H., Koistinen, J., and Järvinen, H. 2010. Quality Assurance in the FMI Doppler Weather Radar Network. Boreal Environment Research. 15: 579–594.

Schär, C., Ban, N., Fischer, E. M., Rajczak, J., Schmidli, J., Frei, C., Giorgi, F., Karl, T. R., Kendon, E. J., Tank, A. M., O'Gorman, P. A., Sillmann, J., Zhang, X., and Zwiers, F. W.: Percentile indices for assessing changes in heavy precipitation events, Climatic Change, 137, 201–216, https://doi.org/10.1007/s10584-016-1669-2, 2016.

Tamm, O., Saaremäe, E., Rahkema, K., Jaagus, J., and Tamm, T. 2023. The intensification of short-duration rainfall extremes due to climate change–Need for a frequent update of intensity–duration–frequency curves. Climate Services. 30: 100349.

Taylor, K. E., Stouffer, R. J., and Meehl, G. A. 2012. An overview of CMIP5 and the experiment design. Bulletin of the American meteorological Society. 93: 485–498.

Termonia, P., Fischer, C., Bazile, E., Bouyssel, F., Brozková, R., Bénard, P., Bochenek, B., Degrauwe, D., Derková, M., El Khatib, R., *et al.* 2018. The ALADIN System and its canonical model configurations AROME CY41T1 and ALARO CY40T1. Geoscientific Model Development. 11: 257–281.

Van Vuuren, D. P., Edmonds, J., Kainuma, M., Riahi, K., Thomson, A., Hibbard, K., Hurtt, G. C., Kram, T., Krey, V., Lamarque, J.-F., *et al.* 2011. The representative concentration pathways: an overview. Climatic change. 109: 5–31.

Venäläinen, A., Jylhä, K., Kilpeläinen, T., Saku, S., Tuomenvirta, H., Vajda, A., and Ruosteenoja, K. 2009. Recurrence of heavy precipitation, dry spells and deep snow cover in Finland based on observations. Boreal environment research. 14: 166.

Wilks, D. 2016. “The stippling shows statistically significant grid points”: How research results are routinely overstated and overinterpreted, and what to do about it. Bulletin of the American Meteorological Society. 97: 2263–2273.